

PHYSICAL REVIEW A

GENERAL PHYSICS

THIRD SERIES, VOLUME 40, NUMBER 10

NOVEMBER 15, 1989

Precision measurement of the orthopositronium vacuum decay rate using the gas technique

C. I. Westbrook,* D. W. Gidley, R. S. Conti, and A. Rich

Department of Physics, University of Michigan, Ann Arbor, Michigan 48109

(Received 1 June 1989)

The vacuum decay rate λ_T of orthopositronium (1^3S_1) formed in a gas has been measured to be $\lambda_T = 7.0514 \pm 0.0014 \mu\text{s}^{-1}$. Measurements of λ_T in four different gases, all in agreement, are averaged to obtain this result. As systematic tests, two entirely separate digital timing systems are simultaneously used throughout the experiment; the cross section for collisional quenching of the long-lived 2^3S_1 excited state is determined; λ_T is redetermined in two of the gases (N_2 and Ne) using only high-gas-density measurements; and the collisional quenching rate of water vapor, the major residual gas contaminant, is directly measured. The final value of λ_T from this gas experiment, which represents a factor of 4 improvement in accuracy over previous measurements, is 9.4 experimental standard deviations above the theoretical value.

I. INTRODUCTION

Positronium (Ps), the bound state of the electron and positron, is a purely leptonic state—it is effectively free of hadronic and weak-interaction effects. As such Ps is an attractive testing ground¹ for quantum-electrodynamics (QED) calculations and, in particular, for testing relativistic bound-state formalism in quantum field theory.^{2,3} One of the most interesting and fundamental properties of Ps is its decay by annihilation into two or more photons. The possibility of annihilation into γ rays is unique among the atomic systems used to accurately test QED. Precision measurement of the Ps ground-state triplet (1^3S_1) decay rate, λ_T and the singlet (1^1S_0) decay rate, λ_S represent the most rigorous check on any decay rate calculations to date. The triplet state, with lifetime $\lambda_T^{-1} \approx 140$ ns, is more readily measured with high precision because it lives 10^3 times longer than the singlet state. Thus, while there is only one precision measurement⁴ of λ_S there were four of λ_T published prior to 1987 (see Table I). At that time we reported in a paper⁸ the re-

sult of an improved measurement of λ_T in three different gases: isobutane, neopentane, and nitrogen. While the earlier results shown in Table I are 1–2.5 standard deviations above the theoretical value, the 1987 result exceeds theory by 10 standard deviations and is still in agreement with the previous measurements. At the same time that this 200 ppm measurement was published, a new 1000 ppm measurement⁹ of λ_T appeared as shown in Table I.

In this paper we present a more detailed discussion of the 1987 measurement of λ_T which includes a complete reevaluation of the data-analysis procedure. Particular emphasis is given to recent systematic tests and a careful evaluation of systematic errors. In addition, we present a new measurement of λ_T in a fourth gas, neon, that is in agreement with the results from the other three gases.

II. THEORY

Triplet Ps decays via the electromagnetic interaction into an odd number of photons greater than one since even numbers of decay photons are forbidden by charge conjugation invariance and one photon decay violates momentum conservation. The theoretical value of λ_T may thus be expressed as

$$\lambda_T = \lambda_3 + \lambda_5 + \lambda_7 \cdots,$$

where λ_3 is the decay rate into three photons, λ_5 the decay rate into five photons, etc. The value of λ_5 has been calculated¹⁰ to be $\lambda_5 \sim 0.18(\alpha/\pi)^2\lambda_3$ and is thus negligible at the levels of precision discussed herein. At the 10 ppm level it is sufficient to concentrate on λ_3 , which may be expressed as

TABLE I. The most recent measurements of λ_T .

λ_T (μs^{-1})	Date
7.056 ± 0.007	1978, Ref. 5
7.045 ± 0.006	1978, Ref. 6
7.050 ± 0.013	1978, Ref. 7
7.051 ± 0.005	1982, Ref. 4
7.0516 ± 0.0013	1987, Ref. 8
7.031 ± 0.007	1987, Ref. 9

$$\lambda_3 = \frac{2(\pi^2 - 9)}{9\pi} \frac{\alpha^6 mc^2}{\hbar} \left[1 + A_3 \left(\frac{\alpha}{\pi} \right) - \frac{1}{3} \alpha^2 \ln \alpha^{-1} + B_3 \left(\frac{\alpha}{\pi} \right)^2 \dots \right]. \quad (1)$$

The leading term was first calculated in 1949 by Ore and Powell.¹¹ The two most recent calculations of A_3 yield $A_3 = -10.266 \pm 0.011$ (Ref. 12) and $A_3 = -10.282 \pm 0.003$.³ The coefficient B_3 is still uncalculated and, if it is of order unity, this term would only produce a 5 ppm contribution to λ_3 . It may be more appropriate¹³ to write this second-order term as $B_3' \alpha^2$, for which a coefficient of unity would produce a 50 ppm effect. Including the term in $\alpha^2 \ln \alpha^{-1}$ (Ref. 12) and the more accurate A_3 coefficient, then $\lambda_3 = 7.03830 \pm 0.00005 \mu\text{s}^{-1}$. Terms of order α^2 with unit coefficients would contribute $\pm 0.0004 \mu\text{s}^{-1}$.

III. EXPERIMENTAL TECHNIQUE

A. Overview

The technique used in this experiment is similar to that used in Ref. 4. Positrons from the β decay of a radioactive source are stopped in a gas and form *o*-Ps with roughly 25% efficiency. The start signal for a time-to-digital converter (TDC) is provided by the detection of the emitted β particle. When the Ps decays, its annihilation γ rays are detected to provide a TDC stop. The data consist of a histogram of start-stop time intervals. A drawing of the apparatus is shown in Fig. 1. The entire

interaction region is in a 6.8 kG magnetic field which increases the signal rate by causing all positrons with a forward momentum component to follow helical paths through the region viewed by the detectors. The magnetic field mixes the $m=0$ magnetic substates¹⁴ giving rise to perturbed singlet and triplet decay rates which correspond to lifetimes of 0.12 and 13 ns, respectively, in a field of 6.8 kG. The decay rate of the $m=\pm 1$ states, however, remains at λ_T . The value λ of the decay rate of *o*-Ps at a particular gas density can be measured by fitting a single exponential function to the TDC spectrum provided that one begins the fit at a late enough time (typically 150 ns) so that the perturbed triplet component has decayed away sufficiently. The value of λ is always higher than that of λ_T due to collisional "pickoff" of Ps with the gas atoms. The value of λ_T is found by linearly extrapolating the measured λ 's at different gas densities to zero density. Measurements of λ_T in four different gases, isobutane (C_4H_{10}), neopentane (C_5H_{12}), nitrogen, and neon will be presented. For a more detailed discussion beyond that presented in this paper, see the thesis of Westbrook.¹⁵

B. Apparatus

A cylindrical brass chamber of diameter 7.5 cm and length 14 cm is placed in the gap of a Varian-type V-4201-3B electromagnet (see Fig. 1). At one end of the chamber is a 10- μCi ^{22}Na β positron source with a diameter of 2–3 mm. The source is deposited as NaCl onto a 0.125-mm-thick plastic scintillator (Nuclear Enterprises NE 104). The light from the scintillations is guided by acrylic light pipes to an Amperex XP2020 photomultiplier tube (PMT) about 60 cm away from the source region. Typical pulse heights for positron scintillation events are about 2–3 photoelectrons. This "start" detector has a detection efficiency for the forward-going β particles of approximately 50%. The "stop" detector consists of two semiannular pieces of Pilot B scintillator which surround the gas chamber. Their inner and outer diameters are 8.6 and 33 cm, respectively. Two Hamamatsu R1250 PMTs are connected to each half of the annulus by 11-cm-diam, 85-cm-long acrylic light pipes. The outputs of the four phototubes are summed in a dc analog mixer before being pulse-height discriminated. The combined detection efficiency for a three-photon Ps decay is 25%–50%, depending on the discriminator setting. Inside the vacuum chamber, surrounding the source is a tungsten annulus which shields the stop scintillators from the radiation emitted by the ^{22}Na source. At the other end, another tungsten annulus acts as a "beam dump" for positrons which pass through the gas without stopping. The end of the chamber has several layers of Pb foil glued in place to help reflect high-energy positrons back into the interaction region if they do not stop on the first pass.

The brass chamber containing the gas was connected through copper tubing to a 4-in-diam NRC diffusion pump and to a manifold through which various gases could be admitted to the chamber. After several days of pumping the pressure measured by an ionization gauge in

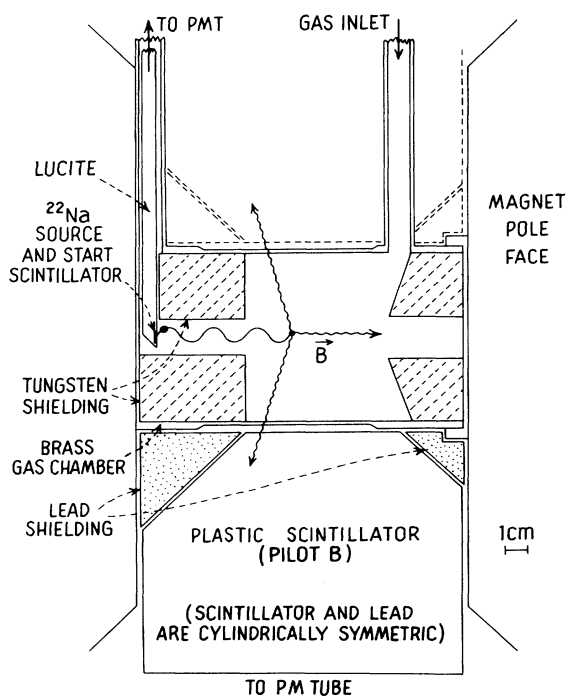


FIG. 1. Ps formation chamber and detector arrangement.

the system read $(2-6) \times 10^{-7}$ Torr. During most runs the chamber was pumped out each day to about 5×10^{-6} Torr and flushed with fresh gas before being refilled. The gas pressure was measured by a calibrated Baratron capacitive manometer (type 170M-6B). This manometer was in the vacuum system at all times and could continuously monitor the gas pressure. The temperature was monitored by two Hewlett-Packard thermistors (model 44414A) whose resistance was read by a digital multimeter. One of these thermistors was taped directly to the 1-mm-thick wall of the Ps interaction region, the other was taped to an arm of the gas handling manifold which effectively monitored the laboratory air temperature. Pressure and temperature measurements were recorded hourly. Tests indicated that the maximum "leak-up" rate, due to either external leaks or outgassing (the system was not bakable) while the vacuum system was not being pumped was 0.1 Torr/day. Residual-gas analysis revealed that the leak-up gas contained chiefly H_2O , CO , and CO_2 . Less than 2% O_2 was observed.

For the runs using N and Ne gas, it was necessary to use a 10–30 Torr admixture of either isobutane or neopentane as a quench gas. The quench gas causes low-energy positrons that have fallen below the Ps formation threshold to rapidly annihilate. Unquenched positrons can live for hundreds of ns in N and Ne. The gases were mixed by first admitting the quench gas and then the other gas. The combination was mixed thoroughly by using a diaphragm-type pump to circulate the gas in a loop around the gas chamber. Monitoring the annihilation rate of the low-energy positrons was used to demonstrate that gases had been thoroughly mixed. A leak of about 0.05 Torr/h was observed in the pump during its operation. To prevent this leak from contaminating the gas, it was sealed off from the rest of the chamber except during mixing, which typically lasted 10 min.

The gas density was computed from the pressure and temperature measurements using the ideal gas law with, when necessary, a first virial correction. At the temperatures in this experiment, 20–25 °C, the virial coefficients of isobutane and neopentane are -0.625 ± 0.060 and -0.90 ± 0.09 l/mol, respectively (see Refs. 15 and 16 for a discussion of these values). The virial coefficients for N and Ne mixed with small amounts of isobutane or neopentane are negligible in this experiment.

C. Electronics

Because of their importance in the analysis of the data and because of their complexity, the electronics will be discussed in some detail. The timing pulses from the β PMT were sent into a differentiating amplifier (Ortec model 454) to be converted to bipolar pulses before being pulse-height discriminated by an Ortec model 583 discriminator using leading edge timing. The γ pulses were discriminated by a LeCroy model 821 discriminator, again using leading edge timing. After the β and γ discriminators, the signals were processed by two completely independent digital timing systems. One of the two systems employed a LeCroy model 4204 TDC, which with its 1-MHz start-rate capability, permitted a very simple electronic setup as shown in Fig. 2. The outputs from

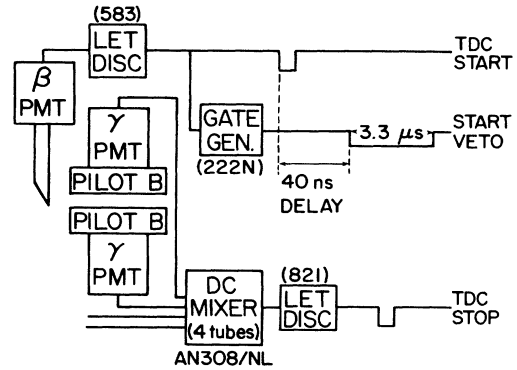


FIG. 2. Electronics for the fast system. DISC stands for discriminator (with leading-edge timing).

the discriminator were sent directly to the TDC inputs. The veto pulse prevents synchronization between start and stop pulses.¹⁷ Valid start rates (the rate at which the TDC digitizing cycle was initiated) as high as 100 kcps were used in this "fast system."

Assuming that the perturbed triplet component has decayed away, the shape of the histogrammed TDC spectrum for the fast system has, to sufficient accuracy, the following form:^{17,18}

$$N(t) = (Ae^{-\lambda t} + B + Ce^{-2\lambda t})e^{-Rt}. \quad (2)$$

Here $N(t)\Delta t$ is the rate of counts in a bin centered at time t and of width Δt . If we define R_{o-Ps} to be the detected o -Ps rate, β to be the total start rate, and γ to be the total stop rate, then $A = R_{o-Ps}\lambda$, $B = \beta\gamma$ (assuming $\beta \gg \gamma$), $C = -2R_{o-Ps}^2$, and $R = \gamma$.

The other electronic system employed a much slower (5 kHz) TDC, a Hewlett-Packard 5345A timer-counter. This TDC required a rejection system to filter out as many unwanted events as possible. The logic diagram is shown in Fig. 3. The rejection system requires that any start pulse not be preceded or followed by any other start pulse within $1 \mu s$. It also requires that a stop signal is detected in the interval between 40 ns and $1 \mu s$ in order for the start signal to be sent to the TDC. In addition, a deadtime of $1 \mu s$ was imposed on the stop. The valid start rate in this "slow system" was thereby reduced to approximately 1–2 kcps. For this more complex arrangement, the spectrum $N(t)$ is somewhat different. It is shown in Ref. 15 that for the slow system, A in Eq. (2) is unchanged, $B = \beta\gamma_u$ (γ_u is the uncorrelated stop rate, i.e., the rate of stops which were not correlated with a start), $C = +0.7R_{o-Ps}^2$, and $R = 0$. These differences are due to the use of the rejection system. The $R = 0$ result is due to the use of a rejection system together with a $1 \mu s$ deadtime per event on the slow system stop discriminator. The uncorrelated stop rate was typically less than 50% of the total stop rate, so that one of the advantages of the slow system was a lower background rate in the spectrum. The term proportional to $e^{-2\lambda t}$ is due to the possibility that two o -Ps atoms could be in the chamber at the same time. The detected o -Ps rate never exceeded

1000 cps in this experiment, therefore, for a fit beginning at 150 ns the component C contributes less than 10^{-4} to the event rate in the first channel, and even less later on. Therefore this component can be neglected for both the fast and slow systems. Higher-order terms due to the presence of three or more o -Ps atoms simultaneously are, of course, also negligible.

Equation 2 was fit to the TDC spectra using a maximum-likelihood routine to extract the parameters A , B , and λ . The parameter R can be measured independently or fit as a fourth parameter. Both methods were used in analyzing the data and a comparison between these two methods is discussed in Sec. V A. One sees that the slow system differed from the fast system in several important ways. In addition to employing a different TDC, it also used much smaller valid start rates, and used different values of the parameters B , C , and R , thereby giving us a check on the theory leading to Eq. (2). The two systems are subject to different systematic errors and therefore the comparison of these two systems constitutes the most rigorous test of the electronics used in this experiment.

The TDC's absolute time calibration was better than 10^{-5} , as measured by an Ortec model 462 time calibrator and by a Monsanto model 3100A frequency synthesizer. The variation in the bin widths, or differential nonlinearity, was carefully measured for each TDC as well. The LeCroy TDC showed fractional variations as large as 3×10^{-3} . The bin widths were measured to a relative accuracy of 1×10^{-4} and were used to correct the data before fitting. Comparison of runs with and without the correction showed less than 60 ppm shifts in the fitted values of the decay rates. The χ^2 of the fit was, however, only acceptable after correction of the data for bin-width variation. The HP TDC showed no significant differential nonlinearity at the 2×10^{-4} level.

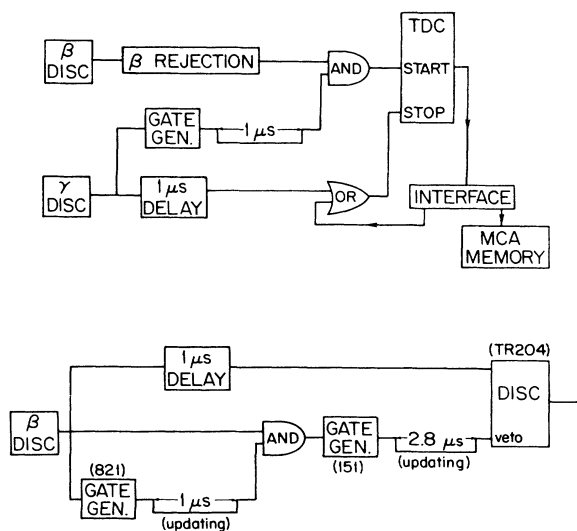


FIG. 3. The electronics for the slow system is shown in the top figure. The box marked β rejection in this figure consists of the β rejection logic shown in the lower schematic.

IV. DATA AND STATISTICAL ERRORS

In typical runs the β rate was 60–120 kcps; the γ rate was an order of magnitude smaller; and R_{o-Ps} was 400–800 cps, depending on the gas composition and density. As a result A/B in Eq. (2), a measure of the signal-to-noise ratio in the experiment, is about 5 for the fast system and 10 for the slow system. Deadtime for the fast system was approximately 25% and for the slow system it was 33%. The stop rate [to be used to determine R in Eq. (2)] was measured at the beginning and end of each day's run. The data used in the fit corresponded to times in the spectrum between 100 and 930 ns. The fit was repeated moving the earliest time out by one bin (8 or 10 ns). The start time t_s of the fitted region was stepped out in this way between 100 and 350 ns after $t=0$. For fits starting at 100 ns, the decay rate is always higher than fits starting at later times. However, in all cases except the lowest pressure Ne and neopentane runs, the fitted decay rate stabilized by $t_s=180$ ns. Thus, rather than trying to determine this time on a run-to-run basis as was done in Ref. 8, the convention was adopted that the decay rate determined by the value of the fit at 180 ns be used in the extrapolation to zero density. As a result the decay rates quoted herein differ slightly from those published in Ref. 8. Because they seemed to take longer to approach their asymptotic value, the lowest pressure Ne and neopentane runs used $t_s=200$ –250 ns.

The fitted values of λ for a given gas density are shown in Table II. The statistical error bar in the table corresponds to the value at t_s . The χ^2 for all the fits beginning at t_s are consistently 100 ± 20 for 100 degrees of freedom indicating that the lifetime spectrum is statistically consistent with Eq. (2) at the 200 ppm level. Also shown in Table II are the slope and zero-density intercept λ_T for a linear fit of λ versus density. These data are displayed in Fig. 4 for each of the four different gases. To arrive at an

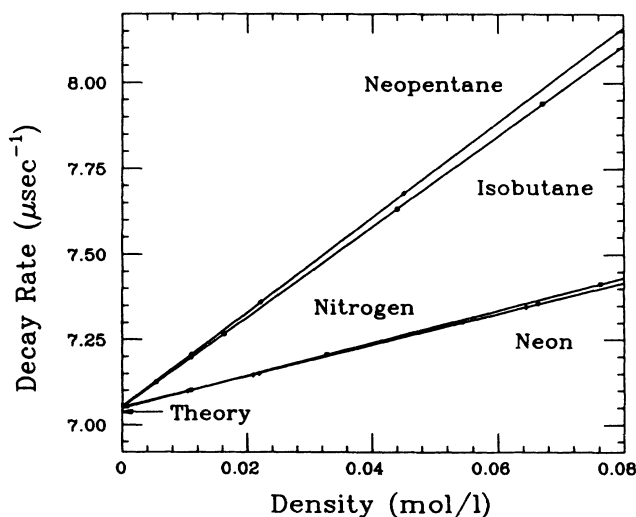


FIG. 4. Plot showing the extrapolation of the observed decay rate in the four gases used in this work. Error bars are approximately the thickness of the line.

uncertainty for the gas density measurements, we have assumed an uncertainty of 0.5 Torr in the average pressure and 1°C in the temperature, both of which we believe to be conservative. The uncertainty in density is converted to an uncertainty in λ by multiplying by the slope of the linear fit versus density. These density-related errors, shown in the last column of Table II, were then added in quadrature to the decay-rate errors to arrive at the total statistical error for each value of λ . We have also performed these extrapolations by using a different fitting routine which treats error bars in both variables. We find negligible shift in the fitted value of λ_T

using this routine. We have also fit the data assuming negligible error in the density extrapolation without shifting the fitted value. The values of λ shown in the table for N and Ne gases have already been corrected for the small effect ($\sim 0.01 \mu\text{s}^{-1}$) of the quench gas. This was done by measuring the partial pressure of the quench gas at the beginning of the run, before the other gas was added, and then using the known slope of the decay rate versus density curve of either isobutane or neopentane, as appropriate, to correct the data. Since the admixtures were small (10–30 Torr) the uncertainties in the correction were negligible.

TABLE II. Observed decay rates for various gas densities of the four different gases used in this work. The column labeled "density error" gives values found by converting the error bar in mol/l to μs^{-1} by multiplying by the slope of the fitted line.

Run name	Density (mol/l)	Slow system (μs^{-1})	Fast system (μs^{-1})	Density error (μs^{-1})
Pure isobutane				
1	5.42	7.124 8(20)	7.125 8(23)	(04)
2	10.94	7.197 8(17)	7.169 7(21)	(06)
3	16.38	7.268 2(14)	7.265 9(14)	(07)
4	16.39	7.267 0(23)	7.267 7(24)	(07)
5	44.14	7.633 4(22)	7.630 1(23)	(17)
6	44.09	7.633 5(25)	7.631 5(30)	(17)
7	67.08	7.939 7(23)	7.939 0(26)	(27)
Fitted λ_T		7.052 6(13)	7.052 1(15)	
Slope m [$\mu\text{s}^{-1}/(\text{mol/l})$]		0.013 19(5)	0.013 15(5)	
χ^2 degrees of freedom		2.6/5	4.8/5	
Nitrogen mixed with 20 Torr of isobutane (extrapolation is in nitrogen density only)				
8	10.97	7.102 6(21)	7.100 9(24)	(02)
9	10.96	7.100 8(25)	7.100 5(27)	(02)
10	32.75	7.206 8(21)	7.203 9(23)	(05)
11	76.23	7.415 1(22)	7.412 9(24)	(11)
Fitted λ_T		7.049 3(18)	7.048 0(20)	
Slope m [$\mu\text{s}^{-1}/(\text{mol/l})$]		0.004 80(4)	0.004 78(5)	
χ^2 degrees of freedom		0.3/2	0.1/2	
Pure neopentane				
12	5.44	7.1290(50)	7.1250(55)	(04)
13	10.99	7.2074(22)	7.2079(22)	(06)
14	22.12	7.3630(32)	7.3585(34)	(10)
15	44.15	7.6788(29)	7.6788(30)	(19)
Fitted λ_T		7.0556(26)	7.0545(27)	
Slope m [$\mu\text{s}^{-1}/(\text{mol/l})$]		0.0138(1)	0.0138(1)	
χ^2 degrees of freedom		0.5/2	1.5/2	
Neon mixed with isobutane or neopentane (extrapolation is in neon density only)				
16	10.39	7.099 0(34)	7.097 9(42)	(02)
17	11.03	7.109 0(42)	7.106 5(48)	(02)
18	20.88	7.144 9(29)	7.141 6(34)	(04)
19	21.85	7.148 9(22)	7.148 9(24)	(04)
20	54.11	7.298 8(20)	7.298 1(21)	(10)
21	66.35	7.356 6(53)	7.357 9(45)	(11)
22	64.45	7.350 3(23)	7.340 2(76)	(11)
Fitted λ_T		7.050 8(23)	7.049 0(26)	
Slope m [$\mu\text{s}^{-1}/(\text{mol/l})$]		0.004 58(6)	0.004 61(6)	
χ^2 degrees of freedom		4.8/5	4.4/5	

V. SYSTEMATIC ERRORS

The systematic errors in this experiment may be divided into two broad categories, those related to the timing electronics, and those related to the gaseous environment in which the Ps exists during its lifetime. Systematic errors in the electronics were studied by making a careful comparison of the two separate electronic systems which were used to collect data simultaneously during the experiment, as well as by comparing runs made under differing conditions. The gas-related systematics are addressed mainly by comparisons of the four independent extrapolations. We discuss these two classes of systematic error in the following sections.

A. Electronics-related systematic errors

A run-by-run comparison of the fast and slow system results revealed a small discrepancy between the measurements made by the two electronics systems. We took the values of $\lambda_{\text{slow}} - \lambda_{\text{fast}}$ for fits to the data between 180 and 930 ns with the value of R held fixed (at the measured stop rate γ) for the fast-system data, and averaged over all the runs at different gas densities. We found a discrepancy of $0.0025 \pm 0.0006 \mu\text{s}^{-1}$. At least part of this discrepancy is related to a small slope of unknown origin observed in the time spectrum of the fast system. This negative slope was measured in "background" runs with no gas in the chamber. Under these conditions A in Eq. (2) is nearly zero, and Eq. (2) predicts a sloping spectrum due to the e^{-Rt} term which appears to be linear for small R . The negative slope appears as an excess in the apparent value of R . We performed background runs and found that the slope in the spectrum corresponded to a value of R which was higher than the value of γ , the actual stop rate, by 350 ± 50 cps. An "excess slope" of 350 cps corresponds to a decrease in the background counting rate per bin of 3.5×10^{-4} over $1 \mu\text{s}$. This effect is correlated with prompt events in the spectrum. It did not appear when completely random stop events were used. The slope was also never observed in the slow system.

The fast-system data were then refit allowing R to be a fourth free parameter. In order to improve the precision for the fitted value of R , the fit was performed to the data between 180 and 2000 ns, rather than the usual 180 to 930 ns. These fits gave a best-fit value of R which was 250 ± 30 cps higher than the measured value of γ when averaged over all the runs. The fitted value of the decay rate was shifted by an average of $(0.0014 \pm 0.0003 \mu\text{s}^{-1})$ compared to the three-parameter ($R = \gamma$ and fixed) fits of the same data. The results shown in Table II are from three-parameter fits of the data between 180 and 930 ns with $R = \gamma + 250$ cps. This correction to R produces an upward shift in λ of $0.0010 \mu\text{s}^{-1}$.

This 250 cps correction to R does not completely remove the discrepancy. Computing $\lambda_{\text{slow}} - \lambda_{\text{fast}}$ for the values tabulated in Table II, we find that a discrepancy of $0.0015 \pm 0.0006 \mu\text{s}^{-1}$ remains. It is possible that our somewhat *ad hoc* correction procedure is incorrect. If the actual correction is 600 cps rather than 250 cps, the fast and slow measurements would be brought into acceptable agreement. However, there may also be nonflat

backgrounds present in the slow system due to its more complicated rejection electronics (see Ref. 15). We cannot rule out such effects in the slow system as a contributor to the above discrepancy.

To further investigate the $\lambda_{\text{slow}} - \lambda_{\text{fast}}$ differences, we did two runs, with source strengths reduced by a factor of 5, which significantly increased the A/B ratio. This should render the effect of nonflat background to be entirely negligible. These runs, 4 and 9 in Table II, had A/B ratios of approximately 35. At these low source strengths, the count rates and deadtimes were such that the two systems had approximately 90% of their events in common, giving a highly reliable comparison between them. Combining runs 4 and 9 we find $\lambda_{\text{slow}} - \lambda_{\text{fast}} = -0.0004 \pm 0.0007 \mu\text{s}^{-1}$. Here, the error bar was determined by adding the standard deviations of the individual runs together in quadrature, and then multiplying by 0.4 to account for their 90% correlation. We see that the discrepancy disappears. Furthermore, runs 4 and 9 agree well with their respective high source strength counterparts. Thus our procedure is summarized as follows. Having identified and applied a 250 cps correction to R for the fast-system data, there is then no reason to favor the results of one system over the other. We therefore averaged the results and assigned a one standard deviation systematic uncertainty of $\pm 0.0008 \mu\text{s}^{-1}$ or half the discrepancy between the two sets of data.

The effect of afterpulsing in the γ PMT's was also carefully examined. The Hamamatsu R1250 tubes used in this experiment showed afterpulses at 500 and 950 ns after the initial pulse. The afterpulse probability was measured to be of order 1×10^{-4} at a reduced discriminator threshold corresponding to three photoelectrons. With such a low discriminator threshold the afterpulses were readily visible in plots of the residuals for the decay rate fits. Approximately 6×10^4 afterpulses were recorded in a 10 day run with deliberately increased afterpulsing. (Note that in order for an afterpulse to appear in a spectrum, it is necessary that the initial pulse be below threshold, otherwise that pulse would have been detected and digitized. Therefore, the afterpulse probability is not the same as the probability that an afterpulse appears in the spectrum, and the latter quantity is the more important one.) The afterpulse probability was reduced by raising the discriminator threshold. At a threshold corresponding to 10 photoelectrons, the afterpulse probability was measured to be 3×10^{-6} . At this threshold level an upper limit of 5000–10000 was placed on the number of afterpulses recorded in the spectrum of comparable length. Adding simulated after-pulses of this intensity to a data run produced a shift in λ of $-0.0003 \mu\text{s}^{-1}$. We therefore place an upper limit of $0.0003 \mu\text{s}^{-1}$ on effects of afterpulsing. In addition runs 5 and 6 provide a comparison of data taken at thresholds of 15 and 10 photoelectrons, respectively. Their agreement supports the above conclusion.

An upper limit of 1×10^{-6} was placed on the afterpulse probability in the β PMT. Furthermore, we know of no reason to expect systematic effects due to afterpulsing in the β PMT's and therefore we do not include it in our error budget.

B. Gas-related systematic errors

There are five main effects that we have considered in this category. They are uncertainties in the value of the virial coefficient B_v of isobutane and neopentane; annihilation of Ps at the brass chamber walls; gas contamination due to leaks or outgassing of the gas system; the formation of long-lived positronium excited states Ps*^{*}; and incomplete thermalization of *o*-Ps which could result in a time-dependent fitted decay rate.

The first of these is easily estimated by performing the fits using different values for the virial coefficient B_v . In the case of isobutane we find a shift of $0.0002 \mu\text{s}^{-1}$ for a change of 10% in B_v . For neopentane a 10% change in B_v produces a $0.0006\text{-}\mu\text{s}^{-1}$ shift. Both of these shifts are negligible compared to the statistical errors.

Since the gas chamber is not of infinite size we must consider the possibility that Ps collisions with the chamber walls might increase λ . The effect should naively be proportional to the chamber's surface-to-volume ratio and to the Ps thermal diffusion length (which should depend on gas density as $1/\sqrt{\rho}$). The probability of quenching at the wall may also be small since Ps decay-rate experiments^{9,17} in evacuated metal cavities show less than 3% increase in λ . We conclude that such wall effects are negligible in the present experiment for two reasons: A detailed study in Ref. 17 was performed in which an aluminum honeycomb was inserted into a gas chamber (with no applied magnetic field). The honeycomb increased the surface-to-volume ratio by a factor of 20–30. In four runs from 100–750 Torr of isobutane no difference was observed in any run at the level of 0.2% and thus the wall effect was assumed to have a one standard deviation upper limit of about 100 ppm. Second, the magnetic field confines Ps formation to the axis of the chamber (see Fig. 1). Thus the experimental upper limit of 100 ppm can probably be reduced by at least an order of magnitude, therefore rendering wall effects negligible in this experiment.

The measured leak-up rate of 0.1 Torr/day in the evacuated gas system can be used to estimate the effects of gas contamination on λ_T . If the residual gas is due to an air leak then the most troublesome gas is the 20% O₂ component. Oxygen would increase the triplet decay rate by $0.046 \mu\text{s}^{-1}/\text{Torr}$ ¹⁹ or about $0.001 \mu\text{s}^{-1}$ after one day if the entire leak-up is air. Residual-gas analysis, however, indicated an upper limit of 2% molecular oxygen in the leak-up gas and thus an upper limit of $0.0001 \mu\text{s}^{-1}$ in the shift in λ_T . As indicated by the residual-gas analysis, water vapor is a major component of outgassing in an unbaked vacuum system. Since we could find no measurements of triplet Ps quenching by water vapor we performed the experiment in our own system. A conflat-flanged water bottle was attached to the gas system and the bottle produced a water-vapor pressure of 15–18 Torr throughout. Approximately 300 Torr isobutane was then quickly dispensed into the system and λ measured over a two day period (with the water bottle attached during the entire run). Comparing λ with our known value of λ at 300 Torr isobutane we find, after three such runs, that the *o*-Ps quench rate of water vapor has an

upper limit of about $0.005 \mu\text{s}^{-1}$ Torr. Thus the effect of water vapor and other gas contaminants is negligible.

The remaining two effects, Ps* formation and Ps thermalization, have to do with the physical interactions between Ps and the various gas molecules. Their effect on the annihilation spectrum are more subtle and difficult to analyze. The constancy of the fitted decay rate between 180 and 350 ns in each typical run and the modest agreement of λ_T in four different gases is the most direct evidence to rule out the possibility that these effects could have produced the 1900 ppm discrepancy with theory which we have observed. These direct comparisons can only place limits of 300–500 ppm on the systematic error. However, as discussed below we believe that effects due to Ps* formation and Ps thermalization can be ruled out at a lower level than this, rendering these effects negligible compared to the statistical uncertainty.

Experiments have shown²⁰ that excited-state yields of as high as 6% of the stopped positron rate are possible in gases. Some of these states have long natural lifetimes. Because of collisions they could have any lifetime shorter than their natural lifetime, and thus could affect the spectrum from which the ground-state triplet lifetime is extracted. In the $n=2$ level the only candidate is the 2*S* triplet state whose natural annihilation lifetime is 1.1 μs . We are able to rule out long-lived 2*S* states as a systematic effect on the basis of an experiment described in the Appendix. We have measured the cross section for deexcitation of the 2*S* state via collisional mixing with the short-lived (3.2 ns) 2*P* states. We find this cross section to be of order 10^{-14} cm^2 . This cross section is similar to that measured in hydrogen.^{21,22} It completely rules out the possibility that 2*S* states can live in 100 Torr of gas for more than a fraction of a ns since the deexcitation rate $n\sigma v$ for thermal Ps* is of order $10^{11}\text{--}10^{12} \text{ sec}^{-1}$.

For Ps* with $n > 2$, the above argument can be extended to the $n=3, 4,$ and 5 states. The radiative lifetimes of the 3*P*, 4*P*, and 5*P* states are short enough that one expects any *S* state to collisionally mix with the short-lived *P* states and disappear quickly compared to 140 ns. This argument does not work for higher n levels because even the *P* states in these levels have long radiative decay lifetimes. The 6*P* state lifetime, for example, is 80 ns. However, there are additional effects in polyatomic gases which will, in all likelihood, cause highly excited Ps* to disappear quickly if it is formed at all and can survive dissociation. An analogous process of collisional, radiationless deexcitation of Na atoms is observed in discharge tubes when small admixtures of polyatomic gases such as C₆H₆ and N₂ are admitted. Cross sections of order 10^{-15} cm^2 are deduced from these observations.²³ It is generally understood that long-range dipole-dipole interactions are responsible for the radiationless deexcitation and the same mechanism will cause deexcitation to the ground state with a similar or even greater cross section.²⁴ This mechanism, in addition to the low probability of highly excited Ps surviving dissociation, removes any concern that Ps* in high- n levels can live longer than about 1 ns at the pressures used in this experiment.

The last gas-dependent effect is associated with the possibility that the velocity distribution of *o*-Ps changes,

i.e., "thermalizes," on a time scale similar to λ^{-1} . In this case, it is possible that λ in Eq. (2) is changing throughout the lifetime spectrum, causing a shift in the fitted lifetime. This effect should be most pronounced at low pressures where the thermalization should be slower. In fact, we observed a trend consistent with thermalization in the fitted decay rate at the lowest pressures used for each gas. As the start channel of the fitting program is successively stepped out beyond $t=150$ ns, the fitted decay rate decreases by roughly 1000 ppm before asymptotically approaching a constant value at 175–275 ns, depending on the gas. An example is shown in Fig. 5. Upon doubling or tripling of the gas pressure, and hence of the Ps-gas collision rate, the effect disappears and λ is observed to be constant beyond 150 ns. We conclude that Ps thermalization effects are negligible at all but the lowest gas pressures used and that, at these low pressures, we have correctly accounted for the effect by selecting the asymptotic value of λ . We therefore expect no pressure dependent shift in the extrapolated value of λ_T .

The thermalization interpretation of the data shown in Fig. 5 is, however, not totally satisfying under closer scrutiny for two reasons. First, a comparison with the data taken in Ref. 4 shows that at 200 Torr of isobutane, the two experiments measured the same value of λ to 300 ppm. In Ref. 4 the fits to the lifetime data were begun at $t=42$ ns, much earlier than in this work. (Note that in this reference the data were taken at three different magnetic field strengths. These were averaged to arrive at the above error bar.) This result indicates that in isobutane the Ps is thermalized to a point where changes in pickoff are negligible in less than 40 ns. If this is true, we have no explanation of the decrease of λ at $t < 180$ ns at low pressures. Second, we would anticipate the polyatomic isobutane and neopentane gases with their vibrational and rotational modes to thermalize Ps more quickly. In a classical sense, the typical mass of the atom struck by the Ps atom should be effectively that of hydrogen in these

gases. However, the Ps thermalization rate is no more than a factor of 2 slower in nitrogen and neon, not a factor of 14 or 20. Only in argon, with atomic mass of 40, did the rate of thermalization appear to be so slow that we abandoned a precision measurement using low pressures (400 Torr or lower). Ps thermalization in argon, however, is certainly not 40 times slower than in isobutane. Thus all the data are not completely consistent with a simple thermalization model. We can effectively dispel concern for this effect by performing the systematic test described in the next section.

C. High gas density extrapolation

The systematic effects discussed above in Sec. III B are most significant at low pressure, i.e., Ps thermalization times and Ps* lifetimes are longer at low gas pressures. In view of the questions regarding thermalization an important test would be to perform the extrapolation in λ using only high pressure (i.e., high density) data. Isobutane and neopentane are not appropriate gases because they liquify at low pressure (~ 3 atm) and have large virial coefficients. Nitrogen and neon are excellent gases for such a test. Since our gas chamber is limited to about two atmospheres we have utilized data published^{25,26} by the positron group (Coleman *et al.*) at University College, London (UCL). They supplied us with lists of λ versus density for N₂ over a pressure range of roughly 7–45 atmospheres (six data points) and for Ne over a pressure range of 22–35 atmospheres (six data points). For N₂ we only used our 1400-Torr result (200 and 600 Torr were eliminated) with the Coleman *et al.* data. The zero-density extrapolation for this high-pressure data is $7.0491 \pm 0.0023 \mu\text{s}^{-1}$ versus $7.0487 \pm 0.0015 \mu\text{s}^{-1}$ using only our low-pressure measurements. For Ne we used our 1000 and 1200 Torr data with the UCL data and the extrapolated result is $7.0496 \pm 0.0035 \mu\text{s}^{-1}$ versus $7.0501 \pm 0.0020 \mu\text{s}^{-1}$ at low pressures. Thus, the zero density intercept is unchanged by eliminating all data acquired below 1000 Torr gas pressure. This result strongly supports our assertion that the effects of Ps thermalization and Ps* formation are negligible (or can be accounted for) throughout the entire pressure range of the present experiment.

VI. CONCLUSION

The measurements of λ_T for each of the four different gases are summarized in Table III. For each gas the value of λ_T in Table II for the slow and fast digitizer systems has been averaged. The error bar in Table III has been reduced only to the extent that each system contributes independent data to the average.

The weighted average of the four values in Table III is $7.0514 \pm 0.0014 \mu\text{s}^{-1}$, where the determination of the error bar is outlined in Table IV and discussed below. The results for the four gases appear to be slightly statistically overdispersive since χ^2 for the weighted average is 7.2 for three degrees of freedom, consistent with a 7% chance that the dispersion is statistical. The neopentane result, which seems to be particularly high, might be the most

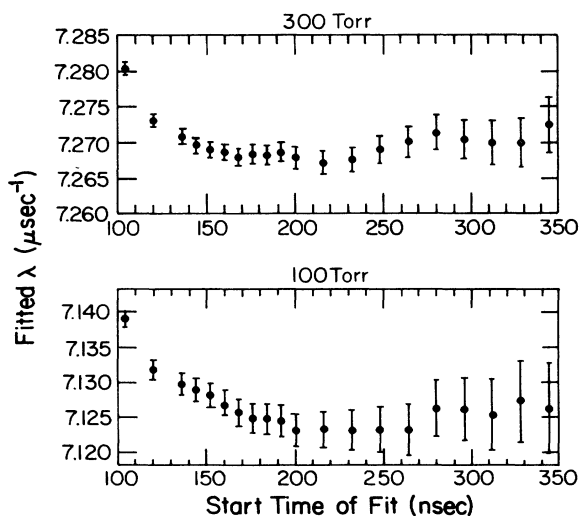


FIG. 5. Fitted decay rates at 100 and 300 Torr of isobutane.

TABLE III. Measurements of λ_T determined by extrapolating to zero gas density in the gas indicated.

Gas	λ_T (μs^{-1})
Isobutane	7.0523 ± 0.0011
Nitrogen	7.0487 ± 0.0015
Neopentane	7.0551 ± 0.0022
Neon	7.0501 ± 0.0020

suspect since we acquired data within 325 Torr of its 1125 Torr liquifaction pressure. However, we saw no indication of anomalous behavior in either the neopentane lifetime spectra or the extrapolation of λ to zero density. Thus, with no real evidence to the contrary, and keeping in mind the limited value of χ^2 as a statistical test when only three degrees of freedom are involved, we will retain the neopentane data in the weighted average.

Since the determination of λ_T in each gas is considered to be a systematic test we do not reduce the statistical error to $0.0008 \mu\text{s}^{-1}$ in the averaging process as would be allowed if the λ_T measurement were known to be independent of gas. Instead we take the statistical error for the isobutane result $0.0011 \mu\text{s}^{-1}$ and combine the systematic errors as shown in Table IV. The final uncertainty is 8% larger than reported in Ref. 8. This is primarily a result of the more extensive analysis of the systematic errors presented here. The difference with theory is 9.4 standard deviations.

The difference with theory could be accounted for if future calculations of the order $(\alpha/\pi)^2$ coefficient, B_3 in Eq. (1), determine it to be of order 300 ± 30 . In light of the large A_3 coefficient, such a result for B_3 is not considered to be so unreasonably large that it can be ruled out a priori.²⁷ There is some theoretical work in progress which is scrutinizing the treatment of the bound-state aspects of the calculation.²⁸ Alternatively, it has been suggested²⁹ that an exotic decay mode of *o*-Ps, not considered in the QED calculation, might explain why the measurement of λ_T is greater than theory. Several axion searches³⁰ can rule out at the 30-ppm level in λ_T all decay processes with a particle and a single photon in the final state. In a separate experiment,³¹ *o*-Ps decay into noninteracting particles was ruled out at the 350-ppm (one standard deviation) level.

Our present 200-ppm measurement of λ_T is in agreement with the earlier 1000-ppm measurements listed in

Table I with the exception of that reported in Ref. 9. The measurement of Ref. 9 agrees with theory at the one standard deviation level but is $(0.020 \pm 0.007) \mu\text{s}^{-1}$ below our new result. The experimental technique is similar to that of Ref. 7 in that Ps is formed in an evacuated confinement cavity. Such vacuum experiments have the important feature that they are subject to very different systematic effects than is the present gas experiment. All gas-related systematics are eliminated. We can offer no explanation of the 3σ difference mentioned above other than to note that, as pointed out in Ref. 9 itself, a complete set of systematic tests were not carried out due to lack of time. We are now acquiring data at the 200-ppm level from an improved vacuum experiment.³² Preliminary results do not support the low value of λ_T reported in Ref. 9.

ACKNOWLEDGMENTS

We thank Alfred Hill posthumously for many discussions concerning positronium decay rate calculations. We acknowledge helpful discussions with P. W. Zitzewitz, J. S. Nico, G. W. Ford, G. P. Lepage, J. Sapirstein, B. Brown, B. Taylor, and K. Eberhart. We thank M. Charlton for kindly supplying us with the UCL decay rate data and S. Hatamian for helping us perform the 2^3S_1 deexcitation experiment discussed in the Appendix. This work was supported by the National Science Foundation under Grant No. PHY8403817 and by the Office of the Vice President for Research of the University of Michigan.

APPENDIX

In an attempt to answer questions about the possibility of excited-state Ps contaminating the TDC spectrum [Eq. (2)] we have undertaken an experiment to measure the collisional deexcitation lifetime of the $2S$ state of Ps. The experiment was performed in a slow positron beam apparatus designed to drive microwave transitions between the 2^3S_1 state and the 2^3P_2 states.

The technique and apparatus of the microwave resonance experiment are described in Ref. 33. Briefly, Ps in the $n=2$ level is formed in a waveguide and a quantity r , defined by

$$r = \frac{R_{\text{on}} - R_{\text{off}}}{R_{\text{off}}},$$

is measured as a function of microwave frequency. Here

TABLE IV. Contributions to the total error assignment in λ_T .

	Error (μs^{-1})	Error (ppm)
Statistics	0.0011	156
Electronics		
Fast-slow difference	0.0008	113
Afterpulsing	0.0003	43
Gas contamination	negligible (see text)	
Virial coefficient	negligible (see text)	
Total	0.0014	200

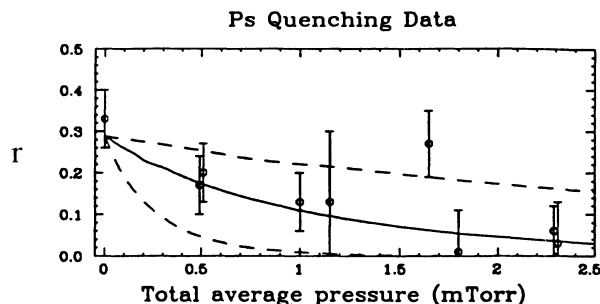


FIG. 6. Data from the collisional deexcitation experiment. The ordinate shows the quantity r as defined in the Appendix. The solid line is the prediction of Eq. (A1) for a cross section $\sigma = 2 \times 10^{-14}$ cm², the dotted lines correspond to values of σ a factor of 4 higher and lower.

R_{on} and R_{off} are the count rates for the $2^3P_2 - 1^3S_1$ decay signal (emission of a Lyman- α photon followed by the characteristic 140 ns 1^3S_1 decay) with the microwaves turned on and off, respectively. When the microwaves are tuned to the $2^3S_1 - 2^3P_2$ resonance frequency (about 8.6 GHz) they cause an increase in the $2^3P_2 - 1^3S_1$ signal. The principle of the collisional deexcitation experiment described below is that if gas collisions can also cause transitions from 2^3S_1 to 2^3P_2 , then the value of r at microwave resonance should decrease with increasing gas density. The dependence of r on density is given by¹⁵

$$r = (1 - e^{-kz}) / (4e^{n\sigma z} - 1), \quad (\text{A1})$$

where z is the distance across the microwave cavity and k is the probability per unit length of a microwave-induced transition. In this experiment $kz \sim 2$, corresponding to a microwave power of 0.5 W/cm².

The experiment was performed by valving off the vacuum pumps and admitting a small amount of N₂ gas into the chamber. Initial pressures ranged from 0–1.5 mTorr. At the highest pressures a 30% attenuation of the incident positron beam was observed. Unfortunately, the vacuum system was outgassing continuously at a rate of 0.1 mTorr/h during the runs of 5–24 h duration. Therefore, our data is contaminated by an amount of CO and CO₂ (detected with a residual gas analyzer) comparable to the initial N₂ density. This prevents us from claiming to have measured the 2^3S_1 deexcitation cross section of a single gas. However, if we make the assumption that σ for N₂, CO, and CO₂ are similar, we may plot the measured values of r versus the average total gas pressure during the run. Such a plot is shown in Fig. 6. The solid line in the figure is the prediction of Eq. (A1) with $\sigma = 2 \times 10^{-14}$ cm², while the dotted lines correspond to values of r a factor of 4 higher and lower. Even if the gases do not have identical deexcitation cross sections, it is clear from Fig. 6 that at least one of these molecules has a very large deexcitation cross section and this lends strong support to the assertion that the $2S$ states are very fragile and will deexcite quickly in the dense gas environment of the o -Ps decay rate experiment.

*Present address: Center for Atomic, Molecular and Optical Physics, National Institute of Standards and Technology, Gaithersburg, MD 20899.

¹For a recent review see A. Rich, R. S. Conti, D. W. Gidley, M. Skalsey, and P. W. Zitzewitz, in *Atomic Physics II*, edited by S. Haroche, J. C. Gay, and G. Grynberg (World Scientific, Singapore, 1989), p. 337.

²G. P. Lepage, *Atomic Physics 7*, edited by D. Kleppner and F. M. Pipkin (Plenum, New York, 1981), p. 297.

³G. S. Adkins, *Ann. Phys. (N.Y.)* **146**, 78 (1983).

⁴D. W. Gidley, A. Rich, E. Sweetman, and D. West, *Phys. Rev. Lett.* **49**, 525 (1982).

⁵D. W. Gidley, A. Rich, P. W. Zitzewitz, and D. A. L. Paul, *Phys. Rev. Lett.* **40**, 737 (1978).

⁶T. C. Griffith, G. R. Heyland, K. S. Lines, and T. R. Twomey, *J. Phys. B* **11**, 743 (1978).

⁷D. W. Gidley and P. W. Zitzewitz, *Phys. Lett.* **69A**, 97 (1978).

⁸C. I. Westbrook, D. W. Gidley, R. S. Conti, and A. Rich, *Phys. Rev. Lett.* **58**, 1328 (1987).

⁹P. Hasbach, G. Hilker, E. Klempt, and G. Werth, *Nuovo Cimento* **97A**, 419 (1987).

¹⁰G. S. Adkins and F. R. Brown, *Phys. Rev. A* **28**, 1164 (1983); G. P. Lepage, P. B. Mackenzie, K. H. Streng, and P. M. Zerwas, *ibid.* **28**, 3090 (1983).

¹¹A. Ore and J. L. Powell, *Phys. Rev.* **75**, 1696 (1949).

¹²W. G. Caswell and G. P. Lepage, *Phys. Rev. A* **20**, 36 (1979).

¹³G. P. Lepage and G. S. Adkins (private communication). This modification was suggested since bound-state corrections of

order α^2 will occur as well as radiative corrections of order $(\alpha/\pi)^2$.

¹⁴O. Halpern, *Phys. Rev.* **94**, 904 (1954).

¹⁵C. I. Westbrook, Ph.D. Thesis, The University of Michigan, Ann Arbor, 1987.

¹⁶J. H. Dymond and E. B. Smith, *The Virial Coefficients of Gases and Mixtures* (Oxford, New York, 1980).

¹⁷D. W. Gidley, Ph.D. Thesis, The University of Michigan, Ann Arbor, 1979.

¹⁸R. A. Lundy, *Phys. Rev.* **125**, 1686 (1962).

¹⁹M. Charlton, *Rep. Prog. Phys.* **48**, 737 (1985).

²⁰G. Laricchia, M. Charlton, G. Clark, and T. C. Griffith, *Phys. Lett.* **66**, 6 (1970).

²¹W. L. Fite, R. T. Breckman, D. G. Hammer, and R. F. Stebbings, *Phys. Rev.* **116**, 363 (1959).

²²F. W. Byron, R. V. Krotkov, and J. A. Medeiros, *Phys. Rev. Lett.* **24**, 83 (1970).

²³For a wide range of excited-state atomic-quenching cross sections, see H. S. W. Massey, E. H. S. Burhop, and M. B. Gilbody, *Electronic and Ionic Impact Phenomena* (Clarendon, Oxford, 1971), Vol. 3, pp. 1656–1696.

²⁴G. W. Ford (private communication).

²⁵P. G. Coleman, T. C. Griffith, G. R. Heyland, and T. L. Killeen, *J. Phys. B* **8**, 1734 (1975).

²⁶P. G. Coleman, T. C. Griffith, G. R. Heyland, and T. L. Killeen, *Atomic Physics 4*, edited by G. Zuputlitz, E. W. Weber and A. Winnacher (New York, Plenum, 1975), p. 355.

²⁷G. P. Lepage (unpublished).

- ²⁸A. Hill, F. Ortolani, and E. Remiddi, in *The Hydrogen Atom*, edited by G. F. Bassani, M. Inguscio, and T. W. Hänsch (Springer-Verlag, Berlin, 1989), p. 240.
- ²⁹J. Cleymans and P. S. Ray, *Nuovo Cimento* **37**, 569 (1983).
- ³⁰U. Amaldi, G. Carboni, B. Jonson, and J. Thun, *Phys. Lett. B* **153**, 444 (1985); W. Wahl, in *Proceedings of the Symposium on the Production of Low-Energy Positrons with Accelerators and Applications*, Giesson, West Germany, 1986 (unpublished).
- ³¹G. S. Atoyan, S. N. Gnimenko, V. I. Razin, and Yu. V. Ryabov, *Phys. Lett. B* **220**, 317 (1989).
- ³²J. S. Nico, D. W. Gidley, P. W. Zitzewitz, and A. Rich, *Bull. Am. Phys. Soc.* **32**, 1051 (1987).
- ³³S. Hatamian, R. S. Conti, and A. Rich, *Phys. Rev. Lett.* **58**, 1833 (1987).